Eur. Phys. J. Special Topics **141**, 181–187 (2007)

DOI: 10.1140/epjst/e2007-00037-7

THE EUROPEAN PHYSICAL JOURNAL SPECIAL TOPICS

Stability of polymer films as a 2D system

Y.J. Wang[1], C.-H. Lam[2,a], X. Zhang[1], and O.K.C. Tsui[1,a]

[1] Department of Physics, Hong Kong University of Science and Technology, Clear Water Bay, Hong Kong
[2] Department of Applied Physics, Hong Kong Polytechnic University, Hung Hom, Hong Kong

Abstract. According to classical theory of phase transition, fluctuations in systems with low dimensions are so violent that the phase boundary between unstable and metastable states would be smeared. In this experiment, we measure the growth of surface fluctuations on an unstable polymer film with a thickness, $h_0 = 5.1\,\mathrm{nm}$, which is much less than the spinodal thickness, $h_{\mathrm{sp}}(= 243\,\mathrm{nm})$ thereby the film is in the very deep unstable region. We find the film to show rupturing behavior markedly different from that of an unstable film. Specifically, nucleation of holes – a characteristic rupturing feature of metastable films – is prominent, which is surprising for a film in the very deep unstable region even provision is given to thin films being two-dimensional and hence are susceptible to broadening of the phase boundary by fluctuations. Monte Carlo simulation shows that the nucleated holes can be caused by stochastic thermal fluctuations. Our result thus confirms the broadening of the phase boundary in thin films by fluctuations to be extremely large. As a consequence, the phase behavior of thin films cannot be predicted by the mean-field calculated phase boundary, which however has been the general practice so far.

1 Introduction

Polymer films are ubiquitous in daily life. Therefore issues concerning their stability are of technological significance. To perceive whether a uniform film would be stable or not, consider a perturbation, $\delta h(\boldsymbol{r})$ to the film profile, where $\boldsymbol{r}$ is a position vector in the film. The resulting change in the system free energy, $\delta\mathcal{G}(h(\boldsymbol{r}))$ is given by:

$$\delta\mathcal{G}(h(\boldsymbol{r})) = \int\ [G(h_0 + \delta h(\boldsymbol{r})) - \mathrm{G}(h_0)]d^2r + \text{surface energy}, \tag{1}$$

where the integration is over the whole film, h_0 is the initial thickness of the film, $G(h_0)$ is the unit-area potential energy. By writing $G(h(\boldsymbol{r}))$ in the Taylor's expansion about h_0, one obtains:

$$\delta\mathcal{G}(h(\boldsymbol{r})) = \int\ [G'(h_0)\delta h(\boldsymbol{r}) + G''(h_0)\delta h(\boldsymbol{r})^2/2 + \cdots]dr + \text{surface energy}. \tag{2}$$

Because of conservation of material mass, the first integral must be zero. It follows that in the long-wavelength limit where the surface energy term is negligible, the lowest order approximation of $\delta\mathcal{G}(h(\boldsymbol{r}))$ is $G''(h_0)\delta h(\boldsymbol{r})^2/2$. Obviously, if $G''(h_0)$ is negative, the film can reduce its energy by increasing $\delta h(\boldsymbol{r})$. This implies instability of the film against spontaneous growth of long-wavelength surface fluctuations. The above discussion provides a heuristic explanation to the conventional approach in assessing the stability of a film: One first hypothesizes the form of $G(h_0)$ for the film system then examine the sign of $\mathrm{G}''(h_0)$ [1–9]. If $\mathrm{G}''(h_0)$ is negative, the film is assumed unstable where the film surface roughens spontaneously according to the so-called

[a] E-mails: phtsui@ust.hk (O.K.C.T.) and C.H.Lam@polyu.edu.hk (C.H.L.)

spinodal mechanism [9–11]. But if $G''(h_0) > 0$, rupturing of the film, if happens, should proceed by the nucleation of holes and the film is assumed metastable. It follows that the spinodal thickness, h_{sp}, where $G''(h_{sp}) = 0$, makes up the phase boundary between unstable and metastable films.

During rupturing, inhomogeneity develops in the local thickness, $h(\boldsymbol{r})$ of the film. By treating h as the order parameter, the rupturing of thin films can be seen equivalent to the phase separation of immiscible binary mixtures. Indeed, the problem of thin film stability and phase transition are equivalent and has been treated in identical way [9, 11]. In classical phase transition theory (and equivalently stability theory of thin films), the calculation is based on a mean-field treatment of the system energy, $\mathcal{G}(h(\boldsymbol{r}))$. That is, $\mathcal{G}(h(\boldsymbol{r}))$ is approximated by $\mathcal{G}(< h(\boldsymbol{r}) >)$, where $\langle h(\boldsymbol{r})\rangle$ means the coarse-grained average value of h about $\boldsymbol{r}$ [12]. Such treatment has an obvious caveat, namely the theory breaks down if the size of the thermal induced fluctuations in the order parameter is comparable to the order parameter at equilibrium (widely known as the Ginzburg criterion [12,13]), which usually occurs when $|h_0 t - h_{sp}|/h_{sp}$ is sufficiently close to zero (where h_0 in this context is the order parameter of the initially uniform system and h_{sp} is the spinodal order parameter) or when the dimension, d of the system is low ($d < 6$ [12–15]) where the influence of thermal fluctuations would be significant. The reason for the anticipated failure of the mean-field theory in the latter case may be envisaged from the fact that in low dimensions fewer neighboring sites are involved in the coarse-grained averaging, rendering the approximation $h(\boldsymbol{r}) \approx \langle h(\boldsymbol{r})\rangle$ vulnerable to statistical fluctuations. In this study, we use atomic force microscopic (AFM) measurements and Monte Carlo simulation to examine the surface fluctuations on polymer films, which is noteworthy a two-dimensional (2D) system.

The organization of this paper is as follows. In Sec. 2, we give the details of the experiment and the Monte Carlo simulation. In Sec. 3, we present and discuss the results on a spinodal unstable polymer film obtained by experiment and simulation. In Sec. 4 we conclude the observations.

2 Methods

2.1 Experiment

Polystyrene (PS) homopolymer with molecular weight 2.3 kg/mol and polydispersity 1.07 was purchased from Scientific Polymer Products. Solution of this polymer in toluene with a concentration of 0.3 wt% was spun-cast at 4000 rpm to produce PS films with thickness equal to about 5 nm. The substrate is silicon covered with a 106 nm thick thermal oxide layer grown by wet oxidation [16]. The thicknesses of the PS films and the oxide layer were measured by ellipsometry. Topographic images of the films during rupture were acquired by a Seiko Instruments SPN3800 atomic force microscope (AFM) operated in the non-contact mode, in which the bright regions represent protrusions and dark regions represent indentations. The annealing temperature was 59°C such that the rupturing rate was convenient for the measurement.

2.2 Monte-Carlo simulation

It is well documented that the polymer film profile $h(\boldsymbol{r}, t)$ evolves according to [1]:

$$\frac{\partial h(\vec{r}, t)}{\partial t} = \nabla \cdot \ [m(h)\nabla p(\vec{r}, t)] + \xi(\vec{r}, t), \tag{3}$$

where the local excess pressure, $p(\boldsymbol{r}, t) = -\gamma \nabla h(\boldsymbol{r}, t) + G'(h)$ and the hydrodynamic conductance, $m(h) = h^3/(12\eta)$. The constants, γ and η denote the surface tension and viscosity of the polymer, respectively. The function, $\xi(\boldsymbol{r}, t)$ denotes the conserved noise arising from thermally activated diffusion of the molecules at the film surface. We assume the potential energy density, $G(h) = -A/(12\pi h^2)$, where A is the Hamaker constant. Linear stability theory predicts that inhomogeneity in $h(\boldsymbol{r})$ would grow spontaneously with time. The growth

involves a fastest growing mode with wavelength, $\lambda_{\rm m} = [-G''(h_0)/2\gamma]^{1/2}$ and time constant, $\tau_m = 48\eta\gamma/\{h^3[G''(h_0)]^2\}$ [9]. In the simulation, we adopt a dimensionless system of units in which $\gamma = \eta = h_0 = 1$. We put $A = 0.032$, which gives $\lambda_{\rm m} = 124.5$. We simulate the dynamics in 2D by numerically integrating eq. (3) by a simple finite difference approach with a unit spatial discretization and a time step of 2. A lattice of width = 1024 with imposed periodic boundary conditions is used. We assume $\xi(x,t)$ to be independent of h. It is implemented by periodically adding to or subtracting from the instantaneous $h(x,t)$ a localized function, $\phi(x - x_0)$, which has zero mean value and random mean position, x_0. We further add a small term, ε/h^8 to $G(h)$ to maintain numerical stability at small h. Each simulation is started with the film initially flat and is stopped when a hole is just nucleated at the substrate. At any instance, the lowest point of the whole film is counted as the bottom of the hole from which the depth is recorded.

3 Results and discussions

Figure 1 shows three AFM topographic images of a rupturing 5 nm film demonstrating its morphologic development in the early stage. As seen, the images display randomly scattered holes in a subtle graininess background in which the length scale increases with time. Previous analysis [17] shows that this graininess background leads to a peak in the 2D Fourier spectrum (with intensity denoted by $|A(q_{\rm max})|$) where the peak position, $q_{\rm max}$, shifts to smaller wave vectors at later times. This observation is consistent with coarsening, which always takes place in the later stage of a spinodal process [9,12]. Here, we focus on the growth of the holes.

Shown in Figure 2(a) is the cross-sectional profile of the #6 hole shown in Fig. 1 at a dewetting time, t, of 1567 s, which is quite representative of the holes we analyzed. We determine the depth, $d_{\rm h}$, for all the holes #1 − #22 at different times and display the result as semi-log plot in Fig. 2(b). In the same figure is displayed $|A(q_{\rm max})|$ vs. time. The slope of this data represents the growth rate, $\Gamma_{\rm m}$, of the fastest mode in the spinodal growth process [9]. As one can see, the majority of the holes initially grow at a similar rate as the spinodal fluctuations do. But at sporadic times, they jump abruptly into full-thickness hole. Since different holes begin to appear at different times, t_0, we re-plot the data of Fig. 2(b) as d_h vs. $t - t_0$ in Fig. 2(c) to compare the jump-in times among the holes. From the new plot, we see that the jump-in times all fall below 2000 s. Since the holes demonstrate no positional order (Fig. 1) and the jump-in times are random (Fig. 2(c)), it has been proposed that the abrupt nucleation of the holes arises from stochastic thermal noises or thermal nucleation [17]. To gain further support to this proposition, and to ensure that the holes do not come from possible heterogeneity of the substrate, we carry out dewetting experiments on a succession of (5 ± 0.5) nm thick PS films deposited on the same oxide-coated silicon substrate, thoroughly washed with toluene between runs to remove the PS residues from the last film. Prior to the experiment, we inscribed a 2 μm (L) $\times$2 μm (W) $\times$ 2 nm (D) indentation in the substrate by focused ion milling. It serves as a marker to enable us to relocate the same region of the substrate to inspect for the rupturing morphology. Figure 3

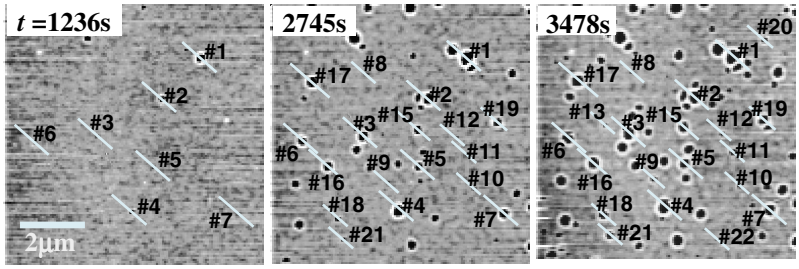

Fig. 1. Topographic images of a rupturing 5 nm PS film obtained by AFM at different times indicated. The numbers gives labels to holes that are later analyzed for the variation of holes depth with time. The scale bar applies to all images.

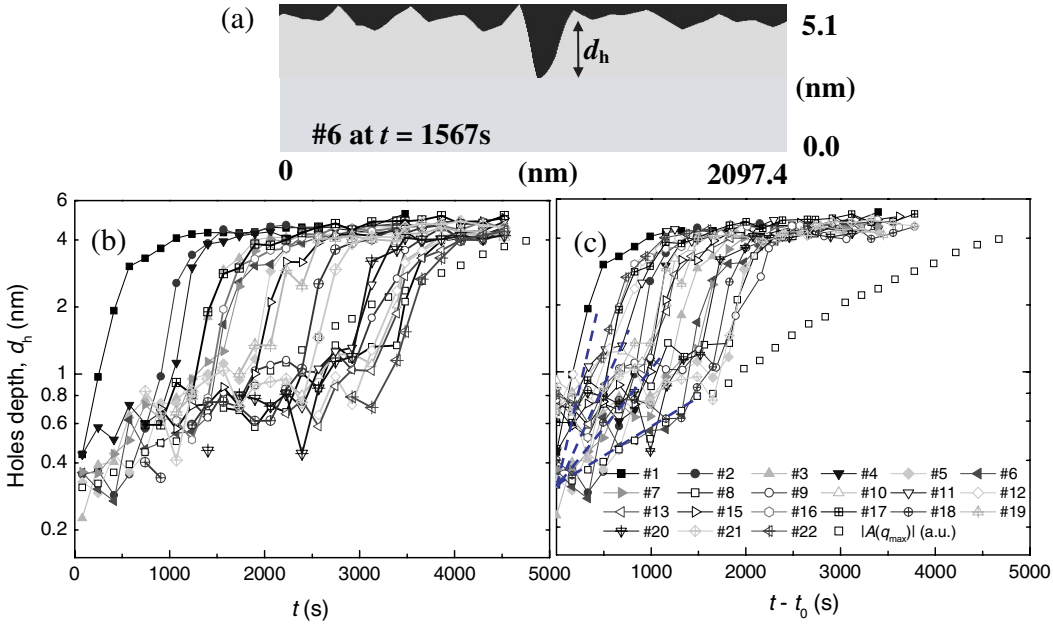

Fig. 2. (a) Cross-sectional profile of the #6 hole at $t = 1567$ s. (b) Semi-log plot of the holes depth, d_h versus dewetting time, t. (c) Similar plot as (b) except that the data is plotted against $t - t_0$, where t_0 corresponds to the time when the hole of interest first appears. The open squares represent the peak height of the Fourier spectrum, $|A(q_{max})|$, plotted as a function of time. The dash lines are straight lines with slopes equal to 1× to 4× of that of the $|A(q_{max})|$ vs. t plot. The legend in (c) applies to (b).

shows representative rupturing morphologies obtained in two representative runs. From these images, it is apparent that the emergence of the holes is uncorrelated in the two runs, supporting the viewpoint that the holes have a stochastic origin.

Next, we examine the results from Monte Carlo simulation. Figure 4(a) shows the profile of a film obtained from three separate simulation runs just before the runs stopped. As seen, the

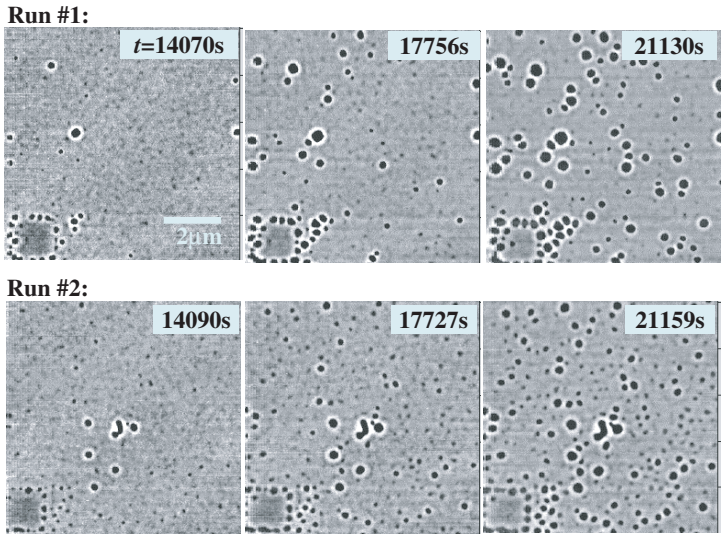

Fig. 3. AFM topographic images obtained from two rupturing (5 ± 0.5) nm PS films at different dewetting times as indicated. The 2 μm ×2 μm square marker can be readily seen on the lower left of each image.

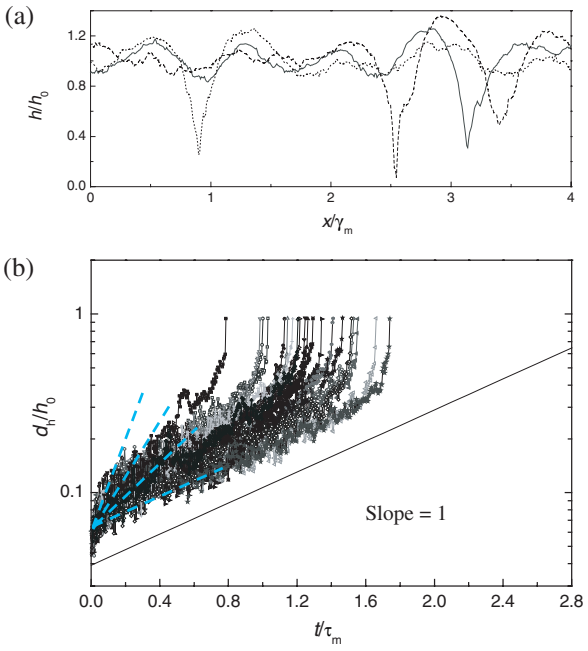

Fig. 4. (a) The simulated profiles of a thickness equal h_0 unstable film obtained from three different Monte Carlo simulation runs. The horizontal coordinate is normalized by the wavelength, $\lambda_{\rm m}$, of the fastest growing mode [9]. (b) Semi-log plot of the normalized holes depth, $d_{\rm h}/h_0$ versus normalized time, $t/\tau_{\rm m}$, for data obtained from twenty simulation runs. The solid line shows the slope 1. The dash lines are straight lines with slopes 1, 2, 3 and 4, respectively.

position of the hole varies in different simulation runs, which is consistent with the result of Fig. 3 that the emergence of the holes in different runs is uncorrelated. Figure 4(b) displays the plot of holes depth vs. time for 20 simulated holes. Overall speaking, it resembles the experimental data in Fig. 2(c). In particular, the simulation shows that the growth of holes changes from linear to super-linear within $t \sim 1.5\tau_{\rm m}$ whereupon the jump-in takes place. This is similar to the experimental observation that the jump-in of holes occurs before $t = 2000\,$s, which is about one $\tau_{\rm m}$ from Fig. 2(c). From Fig. 4(b), the calculation predicts that super-linear growth consistently takes place when the holes depth $d_{\rm h}$ reaches about $0.25h_0$. But the experimental data of Fig. 2(c) shows that super-linear growth commences over a range of $d_{\rm h}$ averaging below 1 nm ($< 0.25h_0$). As mentioned in Sec. 2.2, the simulation assumes $G(h) = -A/(12\pi h^2)$, i.e., the approximated van der Waals (vdW) potential ignoring retardation effects. We examine if the neglect of retardation effects may modify the onset of non-linearity in the fluctuation growth. Recall that $\Gamma_{\rm m} = h^3\,[G''(h)]^2/48\eta\gamma$. To decide when $\Gamma_{\rm m}$ deviates from its value in the initial stage, one much know $G''(h)$. Shown in Fig. 5 (open circles) is a plot of the full

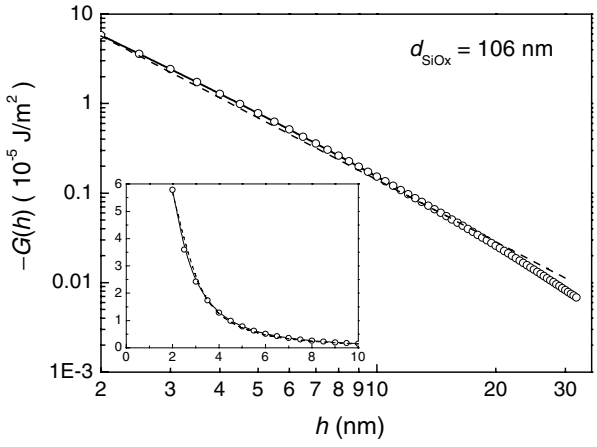

Fig. 5. (Main panel) Log-log plot of the negative of the complete van der Waals potential for the present system, PS-SiO_x-Si, where the thickness of the silicon oxide, $d_{\rm SiOx} = 106\,$nm (open symbols). The dashed line is the best linear fit to the potential in $2 \le h_0 \le 30\,$nm. (Inset) The same data as in the main panel, but plotted in linear scales.

Table 1. Estimated spinodal growth rates for holes with different d_h in a film with average thickness h_0.

d_h/h_0	0.2	0.25	0.3	0.4	0.5	0.6
$\Gamma_m(h_0 - d_h/2)/\Gamma_m(h_0)$ for $G(h) \sim h^{-2.3}$	1.8	2.1	2.5	3.5	5.0	7.4
$\Gamma_m(h_0 - d_h/2)/\Gamma_m(h_0)$ for $G(h) \sim h^{-2}$	1.7	1.9	2.3	3.1	4.2	5.9

vdW potential of the present system, i.e., PS-SiO_x (106 nm)-Si obtained by calculation as detailed in Ref. 18. In the same plot is shown the best linear fit (dashed line) to the calculation. The dashed line, with a slope of − 2.3, clearly provides a good fit. This means that to good approximation $G(h) \sim h^{-2.3}$ and accordingly $\Gamma_m \sim h^{-5.6}$ for $2 \leq h_0 \leq 30$ nm. When a hole is formed, the average local thickness is about $(h_0 - d_h/2)$. By using this approximation, the spinodal growth rate g of holes with different normalized holes depths, d_h/h_0 is estimated. The results are shown in Table 1 for $G(h) \sim h^{-2.3}$ and $\sim h^{-2}$, respectively. As seen, results from the two forms of $G(h)$ agree within 11% up to $d_h/h_0 = 0.4$ where non-linear growth clearly commenced. Hence the use of $G(h) \sim h^{-2}$ in the simulation should not be the cause of the different holes depth found for the onset of non-linear growth in experiment and simulation. The reason for the discrepancy probably comes from inadequacy in the treatment of the noise in the calculation. The present calculation, lacking any element to incorporate the molecular aspects of the polymer, may not be able to simulate the full effects of the fluctuations. Moreover, the noise assumed most probably does not account for the noise engendered by the AFM measurement. According to the simulation result (Fig. 4(b)), the initial growth rate of the majority of holes lies between Γ_m and $\sim 2\Gamma_m$. Apparently, the spinodal growth rate puts a lower bound to the initial growth rate of holes while thermal agitation enables the holes to grow faster. The broader range of initial holes growth rate from Γ_m to $\sim 4\Gamma_m$ found in experiment is thus a manifestation that our model underestimates the stochastic noise. This view is in keeping with the broader range of holes depth found in experiment where non-linear growth commences.

Based on the results presented above, the following picture emerges for the randomized jump-in times of the holes. Essentially, the stochastic noise randomizes the initial growth rate of the holes depth. As the holes deepen enough, non-linear growth takes place causing the ultimate jump-in of the holes. Gray et al. [19] observed nucleation-like growth of random isolated pits in dislocation-free germanium films deposited on silicon. The authors also attributed their observation to the vastly different growth rates of the pits arising from initial randomness that are subsequently amplified by non-linear effects.

We remark that the observed ultimate non-linear growth of a local order-parameter fluctuation should be common to systems with a conserved order parameter close to the spinodal. A conserved order parameter causes the linear term in the system Ginzburg-Landau free-energy functional to be zero. And being close to the spinodal assures that $G''(h_0)$ is small. The two together render the higher-order terms dominant soon after the fluctuations begin to grow. Indeed, off-critical polymer blends are known to phase separate into discrete morphologies [20]. The discrete domains in these morphologies should possess positional order as they are initiated by the spinodal fluctuations. The fact that the holes found here in the 5.1 nm film ($|h - h_{sp}|/h_{sp} = 0.98$) demonstrate no positional order is an indication that thermal fluctuations play a significant role. The vastly different initial holes growth rates revealed by the Monte Carlo simulation is another good indicator that thermal fluctuations are important. In a 11 nm thick film ($|h - h_{sp}|/h_{sp} = 0.95$), which is closer to the spinodal, previous result [8] showed that the plot of $|A(q_{max})|$ vs. t displayed an upturn after the morphology of the film exhibited the standard coarsening, i.e., q_{max} and the growth rate of $|A(q_{max})|$ simultaneously reduced with t. Because the upturn was not found in the $h_0 < 5.5$ nm films, it was seen as a manifestation of the dominance of holes nucleation (i.e., the thermal induced local order-parameter fluctuations) over the spinodal fluctuations. This interpretation is consistent with the result of Balsara et al. [21], who studied phase separation in a metastable polymer blend undergoing nucleation and growth, and found that the $|A(q_{max})|$ vs. t data also displayed an upturn.

4 Conclusions

In conclusion, we have presented results from AFM real-time imaging and Monte Carlo simulation on the growth of surface fluctuations on an unstable film in the deep spinodal region, namely 5.1 nm thick PS film deposited on oxide-covered silicon. Holes were found to occur in the film at random positions and random times. We established that the holes have a stochastic origin and hence attributable to thermal nucleation. Random occurrence of the holes can be understood from a broad dispersal of holes growth rate caused by thermal fluctuations, which are eventually amplified by non-linear effects. Such prominent influence of thermal fluctuations is surprising for a sample far removed from the spinodal as such with $|h - h_{\rm sp}|/h_{\rm sp} = 0.98$ according to the mean-field theory. We propose a connection between this anomaly and the two-dimensionality of a thin film system, under which mean-field theory is known to be vulnerable to fluctuation effects.

One of the authors (O. K. C. T.) is grateful to the support of the Research Grant Council of Hong Kong through the projects HKUST6070/02P and 603604. Another author (C. H. L.) thanks support of the same agency through the project PolyU-5289/02P.

References

1. A. Sharma, R. Khanna, Phys. Rev. Lett. **81**, 3463 (1998)
2. G. Reiter, A. Sharma, A. Casoli, M. David, R. Khanna, P. Auroy, Langmuir **15**, 2551 (1999)
3. R. Seemann, S. Herminghaus, K. Jacobs, Phys. Rev. Lett. **86**, 5534 (2001)
4. R. Seemann, S. Herminghaus, K. Jacobs, J. Phys.: Condens. Matter **13**, 4925 (2001)
5. E. Shäffer, U. Steiner, Eur. Phys. J. E **8**, 347 (2002)
6. B. Du, F. Xie, Y. Wang, Z. Yang, O.K.C. Tsui, Langmuir **18**, 8510 (2002)
7. C. Bollinne, S. Cuenot, B. Nysten, A.M. Jonas, Eur. Phys. J. E **12**, 389 (2003)
8. Y.J. Wang, O.K.C. Tsui, Langmuir **22**, 1959 (2006)
9. Y.J. Wang, O.K.C. Tsui, J. Non-Cryst. Solids (to appear)
10. J.W. Cahn, J. Chem. Phys. **42**, 93 (1965)
11. A. Vrij, J. Th. Overbeek, J. Am. Chem. Soc. **90**, 3074 (1968)
12. P.M. Chaikin, T.C. Lubensky, *Principles of Condensed Matter Physics* (Cambridge University Press, Cambridge, 1995)
13. K. Binder, Phys. Rev. A **29**, 341 (1984)
14. W. Klein, C. Unger, Phys. Rev. B **28**, 445 (1983)
15. Z.-G. Wang, J. Chem. Phys. **117**, 481 (2002)
16. X.P. Wang, X. Xiao, O.K.C. Tsui, Macromolecules **34**, 4180 (2001)
17. O.K.C. Tsui, Y.J. Wang, H. Zhao, B. Du, Eur. Phys. J. E **12**, 417 (2003)
18. H. Zhao, Y.J. Wang, O.K.C. Tsui, Langmuir **21**, 5817 (2005)
19. J.L. Gray, R. Hull, C.H. Lam, P. Sutter, J. Means, J.A. Floro, Phys. Rev. B **72**, 155323-1-155323-11 (2005)
20. H. Chung, R.J. Composto, Phys. Rev. Lett. **92**, 185704 (2004) and references therein
21. N.P. Balsara, C. Lin, B. Hammouda, Phys. Rev. Lett. **77**, 3847 (1996)